Journal of Macromolecular Science, Part A
Publication details, including instructions for authors and subscription information:
http://www.informaworld.com/smpp/title~content=t713597274

Chemorheology and Curing Kinetics of a New RTM Benzoxazine Resin

Qichao Ran[a]; Peiyuan Li[a]; Chi Zhang[a]; Yi Gu[a]
[a] State Key Laboratory of Polymeric Materials Engineering, College of Polymer Science and Engineering, Sichuan University, Chengdu, People's Republic of China

To cite this Article Ran, Qichao , Li, Peiyuan , Zhang, Chi and Gu, Yi(2009) 'Chemorheology and Curing Kinetics of a New RTM Benzoxazine Resin', Journal of Macromolecular Science, Part A, 46: 7, 674 — 681
To link to this Article: DOI: 10.1080/10601320902939598
URL: http://dx.doi.org/10.1080/10601320902939598

Journal of Macromolecular Science®, Part A: Pure and Applied Chemistry (2009) **46**, 674–681

ISSN: 1060-1325 print / 1520-5738 online
DOI: 10.1080/10601320902939598

Taylor & Francis
Taylor & Francis Group

Chemorheology and Curing Kinetics of a New RTM Benzoxazine Resin

QICHAO RAN, PEIYUAN LI, CHI ZHANG and YI GU*

State Key Laboratory of Polymeric Materials Engineering, College of Polymer Science and Engineering, Sichuan University, Chengdu, People's Republic of China

Received January 2009, Accepted February 2009

The chemorheology and curing kinetics of a new high performance resin transfer molding benzoxazine resin was investigated. A chemorheological model based on a modified Arrhenius equation that describes the resin viscosity as a function of temperature and time was proposed. The model, which agreed well with the experimental data, can provide theoretical support for the mold-filling stage in the resin transfer molding process. The average activation energies of the polymerization reaction were obtained by means of gelation times at different temperatures based on the Arrhenius equation and from dynamic differential scanning calorimetry (DSC) results based on the Kissinger and Ozawa methods; the values were 96.0,84.0 and 87.8 KJ/mol, respectively. A plot of activation energy vs. conversion in the curing process was obtained using the Flynn-Wall-Ozawa model. The reaction orders were estimated from isothermal DSC based on a modified Kamal kinetics model which can describe both the autocatalytic and diffusion-controlled curing mechanism.

Keywords: Benzoxazine, RTM, chemorheology, kinetics, model

1 Introduction

Resin transfer molding (RTM), as a liquid composite molding (LCM) process with low cost for producing high performance composites, has received ever increasing attention (1–7). The greatest benefit of RTM is the ability to manufacture large composites with complicated shapes while maintaining the advantage of high-efficiency (8). The RTM process consists of two steps. The first step is the resin injection and fiber impregnation in a heated mold and the following step is the cure of the fiber-resin mixture at an elevated temperature (9). The viscosity and conversion of the resin in the entire process cycle will change with the temperature and time which makes the design and control of the RTM process difficult. To optimize the injection process and shorten the curing time, it is necessary to investigate the chemorheology and curing kinetics of the matrix.

There are many reports about the chemorheology and curing kinetics of the RTM resins (10–15). These studies mainly focus on epoxies, and unsaturated polyester resins and their different curing systems. Because of the special processing characteristics, the matrix for RTM is required to have some features such as low viscosity, suitable pot life, good reactivity and low shrinkage. The main RTM resins are epoxies, unsaturated polyesters, bismaleimides and vinyl esters (16). However, it is difficult to meet the requirements of both easy processing and good properties simultaneously for these resins. So, it is necessary to develop new RTM resins which possess good processing properties and high performance.

Polybenzoxazines (PBZs) are a class of high performance thermoset resins. Benzoxazine precursors possess a number of outstanding properties such as no by-products and near-zero shrinkage during polymerization and good molecular design flexibility (17–20). PBZs have outstanding thermal stability, good mechanical properties, excellent dielectric properties and high char yield (21, 22). All these properties make benzoxazine resins an attractive candidate for RTM (23).

Our research group has prepared a new RTM benzoxazine precursor (BA21). It is based on a modified bifunctional benzoxazine (B-BOZ), with in aldehyde-functional benzoxaizne (Ald-B). Their chemical structures are shown in Scheme 1. BA21 has low melt viscosity (360 mPa·s at 95°C), low curing reactive temperature (with the exotherm maximum at 213°C), and the corresponding polymer has a high T_g (250°C) and high char yield (68.4% at 800°C) (24).

*Address correspondence to: Yi Gu, State Key Laboratory of Polymeric Materials Engineering, College of Polymer Science and Engineering, Sichuan University, Chengdu, 610065, People's Republic of China. E-mail: guyi@scu.edu.cn

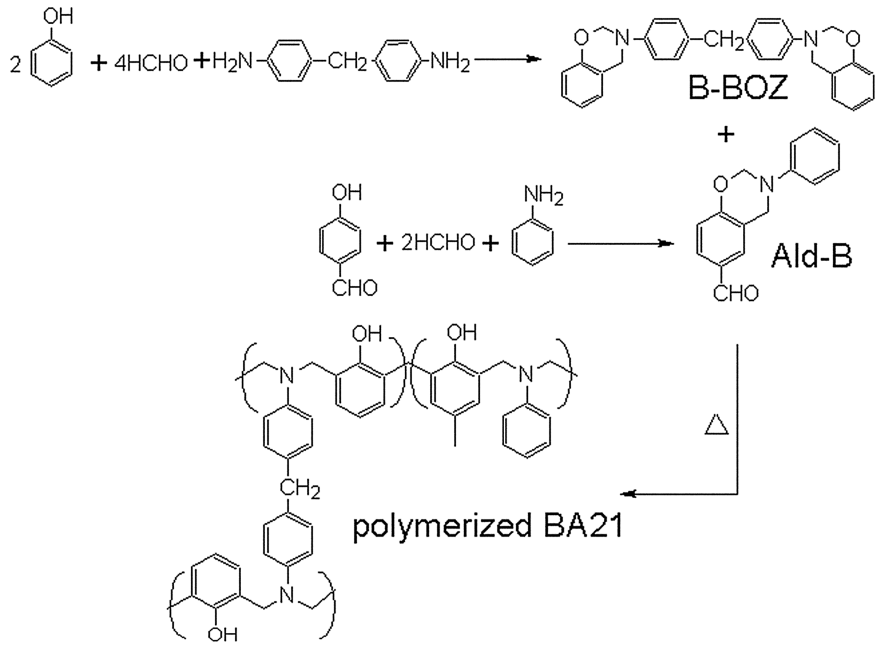

Sch. 1. Chemical reactions to prepare B-BOZ and Ald-B.

The object of the work described in this paper was to characterize and model the chemorheology of BA21 in the injection stage of RTM and the curing kinetics in the curing process with the aim of optimizing the processing schedule.

2 Experimental

2.1 Materials

The benzoxazine monomer B-BOZ was synthesized from phenol, formaldehyde (37% in water) and 4,4′-diaminodiphenyl methane in toluene (19). Ald-B was synthesized from *p*-hydroxybenzaldehyde, formaldehyde (37% in water) and aniline in toluene (25). All chemicals were purchased from the Chengdu Kelong Chemical Reagents Corp (China) and used as received. Both reactions followed the route outlined in Scheme 1. A blend of B-BOZ and Ald-B with the molar ratios 2/1 was mixed in toluene for 10 min. The solution was allowed to evaporate at 85°C under vacuum to remove the solvent. The obtained mixture was designated BA21.

2.2 Measurements

The viscosities of the benzoxazine precursor resins were measured using a Brookfield RVDVII+ Viscometer. Because the resin needs to be degassed to remove any air and residual solvent before injection in the RTM process, the precursor was degassed at 90°C for 30 min. The viscosity vs. temperature was determined from 80 to 165°C at a rate of 1°C min^{-1}, and the values were recorded every five degrees. The viscosities vs. time were determined at 95, 100, 105, 110 and 115°C, and the values were recorded every 10 min.

Gelation times at different temperatures in the range of 160–200°C was measured with a spatula on a steel plate. The steel plate and spatula were heated to a constant temperature. Approximately a 1 g sample was put on the steel plate and spread to a disk with the spatula. Then, the sample was kneaded by pressing it uniformly about every second until the sample was no longer stuck to the spatula. The time was measured and taken as the gelation time of the resin.

DSC experiments were performed using an NETZSCH Instruments DSC 2004 F1. Dynamic DSC was conducted from 60–320°C at rates of 5, 10, 15 and 20°C min^{-1}. In the isothermal DSC experiment, the sample was placed in the cell at a temperature of 120°C; the temperature was then raised quickly to a preset temperature (180, 190 and 200°C) for each isothermal experiment. At the experimental temperature, the instrument needs 5–6 min to achieve stability. The data acquisition was then initiated. After 120 min, the sample was cooled quickly to 100°C. A second scan was then conducted from 100 to 350°C, at a rate of 20°C min^{-1}, to determine the residual heat of reaction (ΔH_{resid}).

3 Results and Discussions

3.1 Viscosity Properties of BA21

For the RTM technique, the initial viscosity of the resin in the injection stage needs to be between 200 and 500 mPa·s (26). Moreover, to assure a complete impregnation of a large product with complicated shape, the viscosity of the

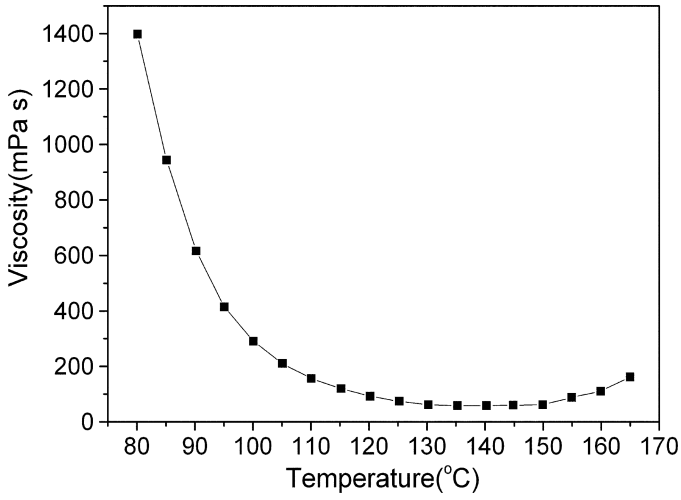

Fig. 1. Viscosity-temperature plot for BA21.

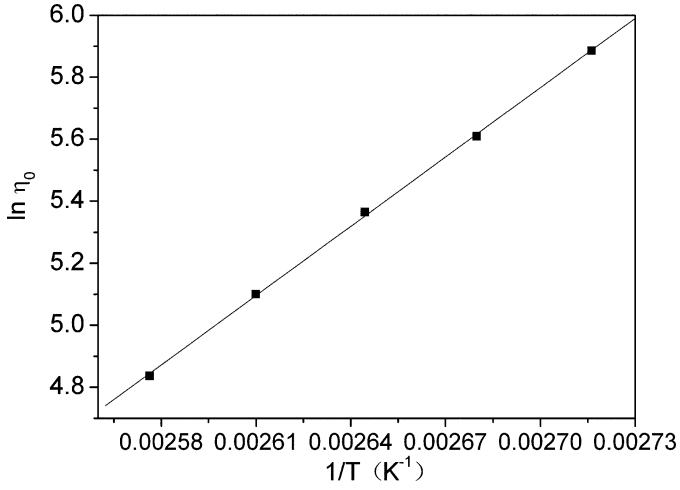

Fig. 3. Model parameters calculation of initial viscosity of BA21.

resin should remain below 1000 mPa·s for at least 300 min; if the viscosity is too high a high injection pressure would be required, which can result in fiber displacements. Figures 1 and 2 are the viscosity-temperature and viscosity-time plots for BA21, respectively. Due to the effect of thermal delay, the initial viscosity in the dynamic test was a little higher than that in the isothermal test at the corresponding temperature. As shown in Figures 1 and 2, to meet the requirements of both low injection viscosity and long pot life, the injection temperature range should be 95–115°C.

3.2 Chemorheological Analysis

The viscosities of thermoset resins are affected by both temperature and the curing reaction. The viscosity initially decreases because of increased thermal effect. As the temperature (or time) increases, the curing reaction begins, the cross-linked network forms, and the viscosity will increase again (27). Both effects can be represented by the following equation (28):

$$\eta(t) = \eta_0 \ \exp(\Phi t) \tag{1}$$

Where $\eta(t)$ is the viscosity as a function of time t, η_0 is the initial isothermal melt viscosity, and Φ is the reaction rate constant. Both η_0 and Φ conform to the Arrhenius equation:

$$\eta_0 = k_1 \ \exp(k_2/T) \tag{2}$$

$$\Phi = k_3 \ \exp(k_4 T) \tag{3}$$

Where k_i(i = 1–4) are the chemorheological parameters, and T is the absolute temperature. When these two Arrhenius equations were directly used to model the chemorheological behavior of this BA21 system, we found the calculated data had some error compared with the experimental results. So, the Arrhenius equation was modified, which can further increase the sensitivity of viscosity to time (29). The modified model used has the form:

$$\eta(t)/\eta_0 = \exp(\Phi t) + \exp(-\Phi t) - 1 \tag{4}$$

To obtain the values of k_1 and k_2 in Equation 2 and the relationship of η_0 and T, Equation 2 is taken in the double-logarithmic form, and can be written as:

$$\ln \eta_0 = \ln k_1 + k_2/T \tag{5}$$

We plotted ln η_0 vs. $1/T$ for the temperatures of 95, 100, 105, 110 and 115°C (Figure 3). By linear regression, the expression of η_0 at different temperatures was obtained:

$$\eta_0 = 5.767 \times 10^{-7} \ \exp\,(7456.330/T) \tag{6}$$

To obtain the value of Φ in Equation 4, we identify $\eta(t)/\eta_0$ as the normalized viscosity and plot $\eta(t)/\eta_0$ vs. t as shown in Figure 4. By multiple nonlinear regressions, the values of Φ at different isothermal temperatures were

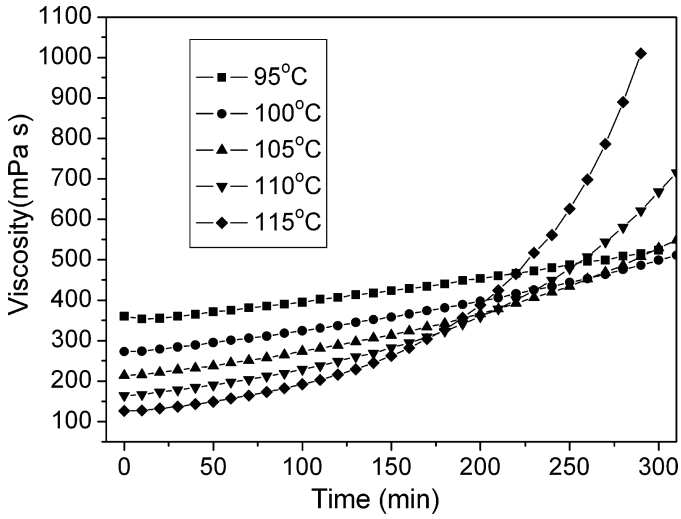

Fig. 2. Viscosity-time plots for BA21 at 95, 100, 105, 110 and 115°C.

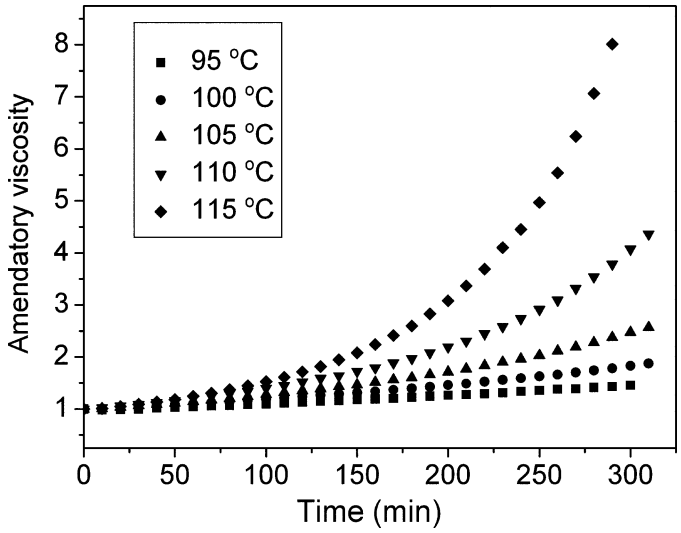

Fig. 4. Normalized viscosity-time plots for BA21.

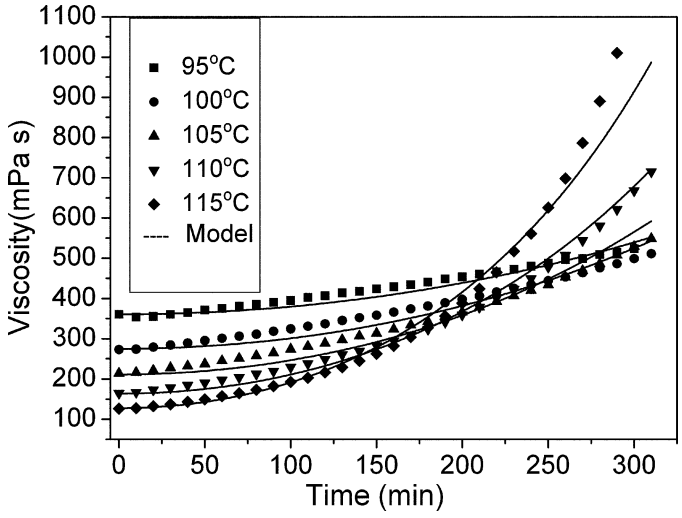

Fig. 5. Comparison of the viscosity model and experimental values at different temperatures.

obtained; they are listed in Table 1. Then, by plotting ln Φ versus $1/T$ and linear regression, the parameter Φ can be described by Equation 7.

$$\Phi = \exp(15.400 - 7905.598/T) \tag{7}$$

Thus, the viscosity of BA21 system can be obtained from Equations 4, (6) and (7) by the following expression:

$$\eta(T,t) = 5.767 \times 10^{-7} \exp\left(\frac{7456.330}{T}\right) \times \left\{\exp\left[\exp\left(15.400 - \frac{7905.598}{T}\right) t\right] + \exp\left[-\exp\left(15.400 - \frac{7905.598}{T}\right) t\right] - 1\right\} \tag{8}$$

To see if the chemorheological model is valid, we compared the calculated data based on Equation 8 with the experimental data (Figure 5). Good agreement in a broad time range was obtained, which means the rheological model based on the modified Arrhenius equation can be used to model and predict the chemorheological behavior of BA21 for the RTM processing window. A Viscosity-temperature-time diagram (Figure 6) in the range of 95–115°C can be obtained based on Equation 8. From Figure 6, one can predict the viscosity of BA21 reached in a certain time and temperature, and choose the suitable injection temperature according to the size and shape of the resulting composite.

Table 1. Parameters of the viscosity model at different temperatures

Temperature (°C)	Φ
95	0.00235
100	0.00307
105	0.00392
110	0.00524
115	0.00718

3.3 Activation Energy

Activation energy (E_a) is denoted as the minimum energy necessary for a specific chemical reaction to occur. The lower the activation energy, the more easily the curing reaction can occur. E_a can be evaluated from the relationship between temperature and time by the measurement of gelation time or the analysis by dynamic DSC.

The gelation activation energy can be determined and calculated based on the gelation times, t_{gel}s, at different

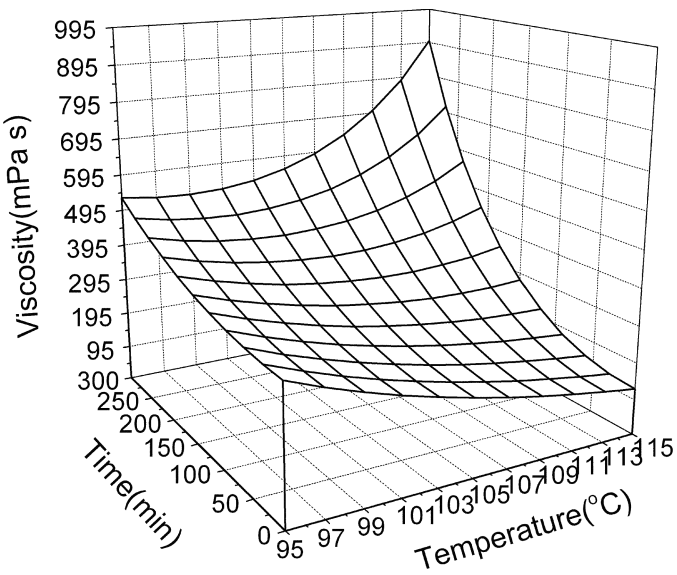

Fig. 6. Temperature-time-viscosity plots for BA21 based on dual-Arrhenius equation.

Table 2. Gelation times of BA21 at different temperatures

Temperature (°C)	t_{gel} *(s)*
160	2670
170	1470
180	855
190	460
200	285

isothermal temperatures with an Arrhenius equation illustrated as follow (30):

$$t_{\text{gel}} = \text{A}\ \exp(\text{E}_\text{a}/RT) \tag{9}$$

Where A is the pre-exponential factor for the reaction, R is the universal gas constant, and T is the absolute temperature. The gelation times of BA21 at different temperatures are listed in Table 2. The apparent activation energy can be obtained from a linear regression of ln t_{gel} vs. $1/T$; the value was 96 KJ mol^{-1}.

Kissinger and Ozawa methods are generally used for the dynamic kinetic analysis when the reaction mechanism is unknown and without assuming any model of kinetic parameters (31, 32). The Kissinger and Ozawa methods can be expressed by Equations 10 and 11, respectively:

$$\ln\left(\beta/\text{T}_\text{p}^2\right) = \ln(AR/\text{E}_\text{a}) - \text{E}_\text{a}/RT_\text{p} \tag{10}$$

$$\ln\beta = \ln(A\,\text{E}_\text{a}/\text{R}) - \text{B} - 1.052(\text{E}_\text{a}/\text{RT}) \tag{11}$$

Where $\beta = dT/dt$ is a constant heating rate, and T_p is the temperature of the exothermic peak.

Figure 7 shows the DSC exothermic peaks for different dynamic heating rates at 5, 10, 15 and 20°C min^{-1}. As the heating rate increased, the exothermic peak shifted to a higher temperature. By plotting ln (β/T_p^2) and ln β vs. $1/T$ (Figure 8), respectively, we obtained the average activation energies; the values were 84.0 and 87.8 KJ mol^{-1}

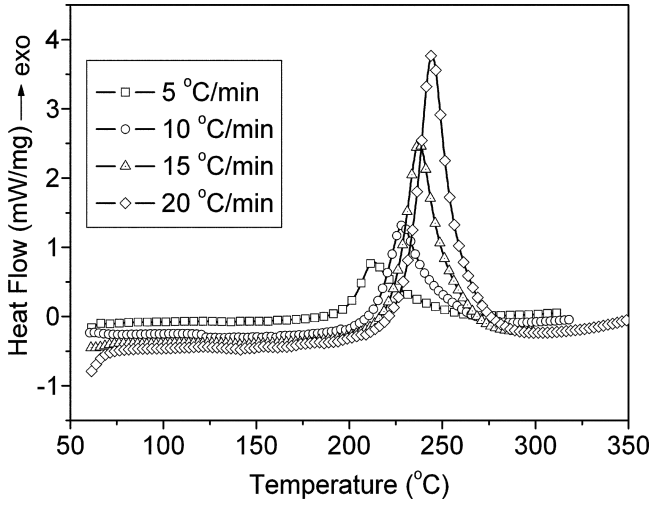

Fig. 7. DSC thermograms of BA21 at different heating rates.

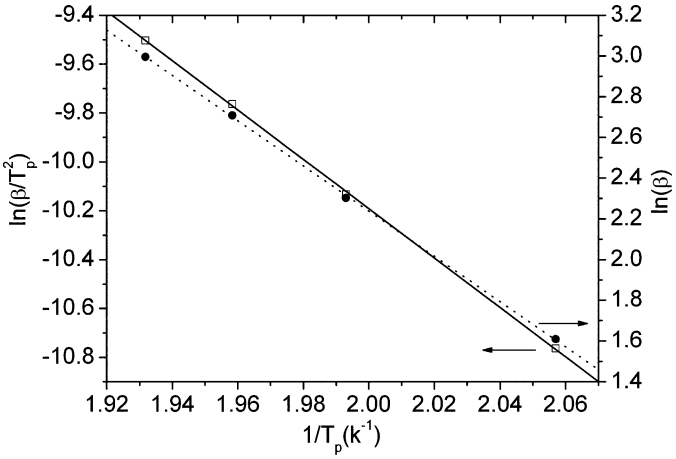

Fig. 8. Kissinger method and Ozawa method plots for averaged activation energy of BA21.

which are not significantly different. However, the values of E_a obtained from dynamic DSC are different from the measurement of gelation time (96 KJ mol^{-1}), which can be explained in that both methods were conducted under different temperature conditions (33). Each gelation time was measured at a constant temperature, while dynamic DSC was performed by a heating technique. The polymerization reactions of benzoxazine resins are non-elementary reactions, and the kinetics mechanism may change with temperature variation.

For use of the above methods to calculate the apparent activation energy, it is assumed that E_a is constant during the entire curing stage and independent of reaction temperature. Actually, E_a is variable. Benzoxazine can be cured via a thermal ring opening reaction to form an analogous phenolic structure. As the extent of curing reaction, α, increases, E_a will change during the curing process. A more complete assessment of the apparent activation energy of BA21 during the curing process can be obtained by isoconversional methods. These methods assume that both the activation energy and pre-exponential factor are functions of the extent of curing. The Flynn-Wall-Ozawa method is one of the isoconversional methods and can be expressed as (32):

$$\ln\beta = \ln(A\,\text{E}_\text{a}/R) - \ln g(\alpha) - 5.331 - 1.052(\text{E}_\text{a}/RT) \tag{12}$$

$$g(a) = \int_0^a \frac{da}{f(a)} \tag{13}$$

Where $g(\alpha)$ is the integral conversion function, and A is the pre-exponential factor for the reaction.

A straight line should be obtained by plotting ln β vs. $1/T$ at a particular conversion α and E_a can be determined from the slope. Figure 9 shows the Flynn-Wall-Ozawa plots of BA21 for $\alpha = 0.2$–0.9, respectively. A good linear relationship was observed. Values of E_a obtained by this method at different conversions are shown in Figure 10. The values

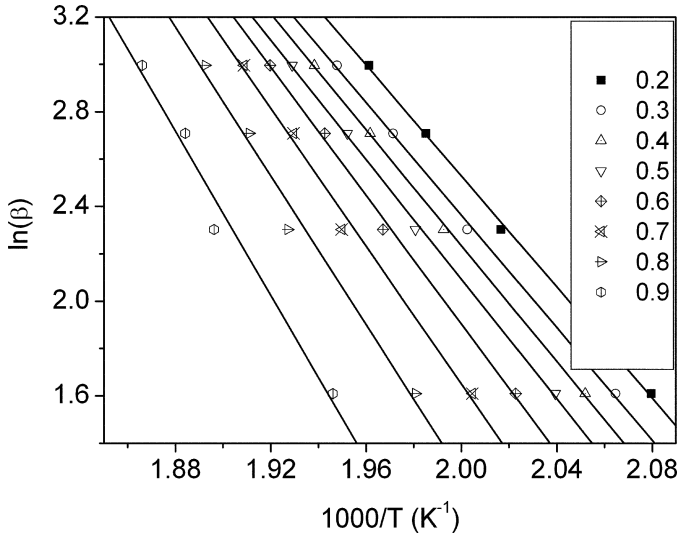

Fig. 9. Flynn-Wall-Ozawa plots at different conversions of BA21: $\alpha = 0.2, 0.3, 0.4, 0.5, 0.6, 0.7, 0.8$ and 0.9.

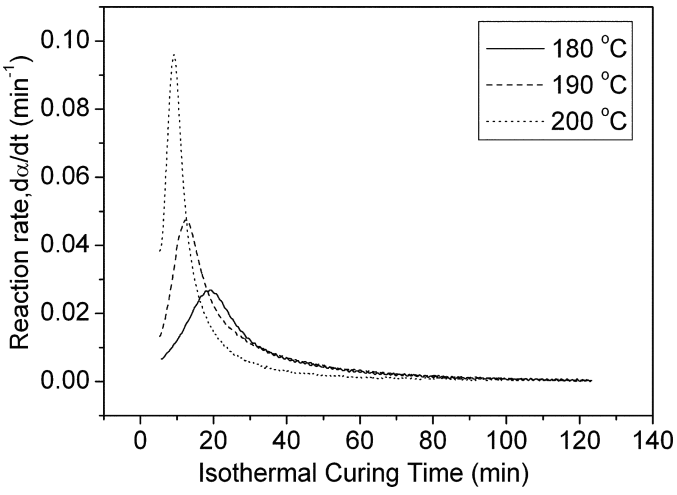

Fig. 11. Reaction rate vs. isothermal curing time at different curing temperatures.

of E_a increase with the increase of the conversions, which is mostly because the formation of the crosslink network makes the curing reactions more difficult.

3.4 Kinetics Analysis

The mechanisms of the curing reactions of thermoset resins commonly include two kinetic reactions, an nth-order and an autocatalytic reaction (12). It has been reported that free phenol groups generated from the ring opening reactions can accelerate further ring opening, which make the curing reactions of benzoxazine resins in the initial stage exhibit the autocatalytic reaction mechanism (34).

Isothermal DSC experiments of BA21 were performed at 180, 190 and 200°C for 120 min. As previously mentioned, the data at the beginning of the isothermal experiment were ignored due to temperature instabilities. The value of the reaction rate ($d\alpha/dt$) at a preset heating temperature and the conversion α reached in time t can be obtained from the following expressions (31, 34):

$$da/dt = (dH/dt)_{\text{iso}}/\Delta H_{\text{tot}} \quad (14)$$

$$\alpha = \Delta H_t/(\Delta H_{\text{iso}} + \Delta H_{\text{resid}}) \quad (15)$$

Where $(dH/dt)_{\text{iso}}$ is calculated from the isothermal DSC curve, ΔH_{tot} is the total heat (276 J g^{-1}) averaged from dynamic DSC at different heating rates, ΔH_t is the heat released until the time t, and can be obtained by integration of the calorimetric signal until time t. ΔH_{iso} is the values

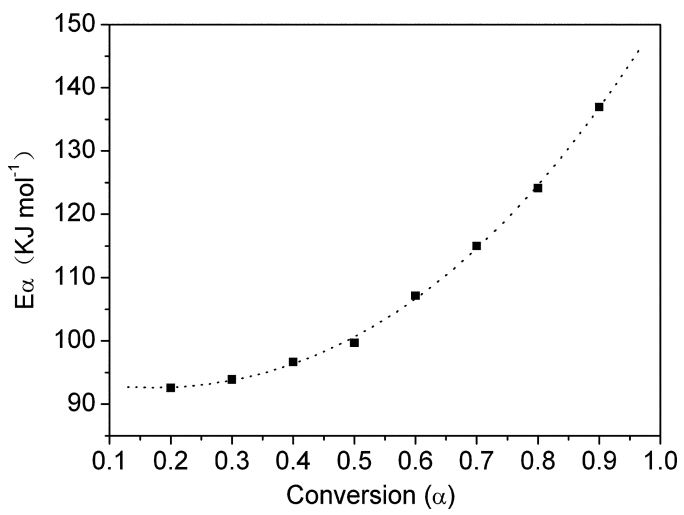

Fig. 10. Values of the apparent activation energy obtained from Flynn-Wall-Ozawa plots at different conversions of BA21.

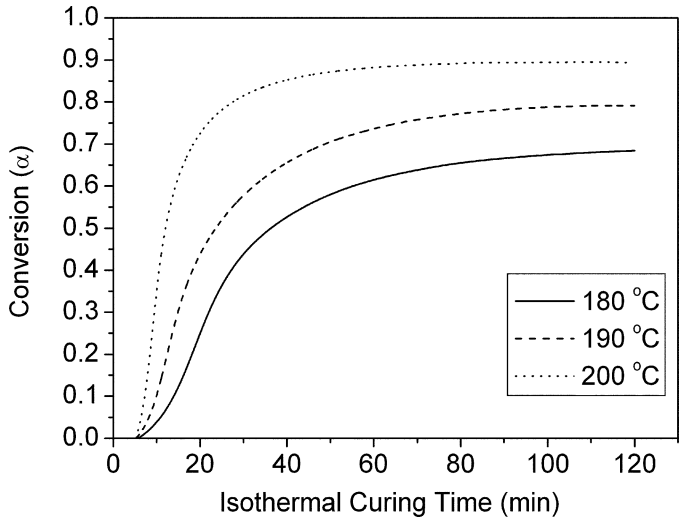

Fig. 12. Conversion vs. isothermal curing time at different curing temperatures.

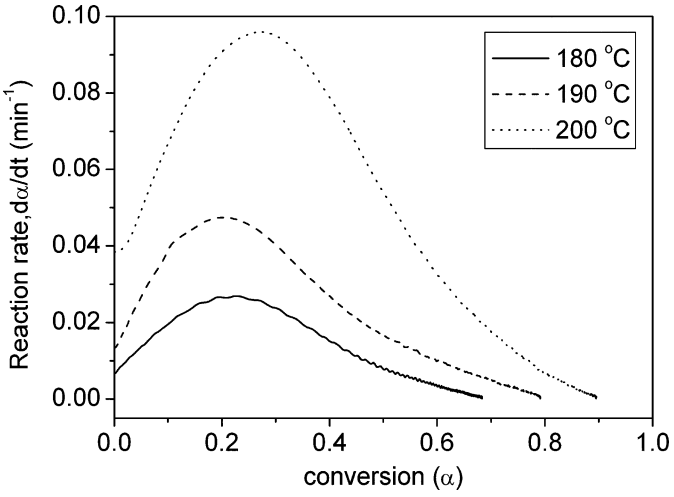

Fig. 13. The tendency of reaction rate vs. conversion.

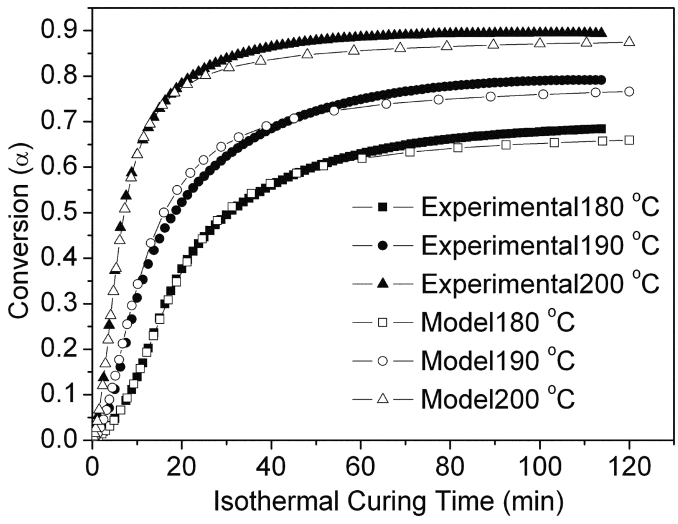

Fig. 14. Comparison of cure kinetics model isothermal conversion predictions with experimental measurement.

of the isothermal heat at each experimental temperature. Figure 11 shows the relationship of $d\alpha/dt$ and t. As expected, the maximum of $d\alpha/dt$ did not occur at time zero, indicating the nature of the reaction is autocatalytic. Additionally, at a higher curing temperature, the reaction rate was higher and the curing time became shorter. Figure 12 illustrates conversion α versus isothermal curing time t at different temperatures. The conversion had a rapid increase at the beginning of the reaction, meaning the crosslink reactions mostly occur during the initial curing stage.

The relationship of $d\alpha/dt$ with α at different curing temperatures is shown in Figure 13. For each curing temperature, the reaction rate exhibited a broad peak and had a maximum of conversion between 0.2 and 0.4, which confirms that the curing process of BA21 follows an autocatalytic reaction (28, 31). According to other authors, the curing reactions of benzoxaizne change from the autocatalytic mechanism in the initial stage to the diffusion-controlled mechanism after vitrification (36). As the curing reactions proceed, the crosslink density of the resin system increases and the molecular mobility is limited, which makes the reaction rate decrease and the increase of the conversion slow. In other words, the conversion can not reach 100% and has a maximum (α_{max}) which is defined as the ratio $(\Delta H_{tot}-\Delta H_{resid})/\Delta H_{tot}$. The $\alpha_{max}s$ of BA21 at 180, 190 and 200°C were 0.68, 0.79 and 0.89, respectively.

In this work, we used the modified Kamal kinetics model (11) which is suitable for both autocatalytic and diffusion-controlled mechanism to study the curing kinetics of BA21:

$$d\alpha/dt = (f_1 + f_2\alpha^m)(\alpha_{max} - \alpha)^n \qquad (16)$$

Where f_1 and f_2 are the model parameters. The reaction orders m and n were estimated without any constraints on them by fitting the experimental data shown in Figure 13 to Equation 16 using a nonlinear regression method. The obtained values of m, n and $m+n$ are shown in Table 3. The overall reaction orders, $m+n$, were 2.5–3.2. The predicted conversion-time plots were obtained using calculated parameters, and compared to the experimental results as shown in Figure 14. Good agreement was observed over the entire curing time for the different temperatures, indicating the chosen kinetics model was valid for the BA21 system.

4 Conclusions

The chemorheological behavior of a RTM benzoxazine BA21 with a low viscosity was investigated based on a modified Arrhenius equation, and the viscosity model was given. The injection temperature range of BA21 should be 95–115°C. Based on this viscosity model, one can choose suitable processing temperatures to meet the requirements of the RTM injection process. The activation energies were determined by different measuring methods and calculated models. The results suggest the activation energy increases with the increase of the conversion. The kinetics behavior of BA21 was described by a modified Kamal model accounting for autocatalytic and diffusion-controlled mechanism, and the overall reaction orders calculated were 2.5–3.2. The maximum conversion of BA21 at 200°C was 0.89 and a complete conversion cannot be reached. The theoretical predictions agree well with the experimental results.

Table 3. Values of m, n and $m+n$ at different curing temperatures

Curing Temperature (°C)	*m*	*n*	*m + n*
180	0.90771	1.85732	2.76503
190	0.63438	1.88215	2.51653
200	1.01997	2.16334	3.18331

The investigations of chemorheology and curing kinetics can provide necessary theoretical parameters for the RTM technique.

Acknowledgments

The authors would like to acknowledge the financial support of the National Natural Science Foundation of China (No.90405001).

References

1. Pillai, K.M. and Advani, S.G. (1998) *Polym. Compos*., 19(1), 71–80.
2. Maazouz, A., Dupuy, J. and Seytre, G. (2000) *Polym. Eng. Sci*., 40(3), 690–701.
3. Yang, H. and Lee, L.J. (2001) *J. Appl. Polym. Sci*., 79(7), 1230–1242.
4. Choi, J.H. and Dharan, C.K.H. (2002) *Polym. Compos*., 23(4), 674–681.
5. Gou, J., Zhang, C., Liang, Z., Wang, B. and Simpson, J. (2003) *Polym. Compos*., 24(1), 1–12.
6. Henne, M., Breyer, C., Michael, N. and Paolo, E. (2004) *Polym. Compos*., 25(3), 255–269.
7. Cheng, Q., Fang, Z., Yi, X.S., An, X., Tang, B. and Xu, Y. (2008) *J. Appl. Polym. Sci*., 109(3), 1625–1634.
8. Yi, X.S. Research and Development of Advanced Composites Technology, National Defense Industry Press: Beijing, China, 84, 2006.
9. Nielsen, D.R. and Pitchumani, R. (2002) *Compos. Sci. Technol*., 62, 283.
10. Naffakh, M., Dumon, M. and Gérard, J.F. (2006) *J. Appl. Polym. Sci*., 102(5), 4228–4237.
11. Lee, C.L. and Wei, K.H. (2000) *J. Appl. Polym. Sci*., 77(10), 139–2148.
12. Yousefi, A., Lafleur, P.G. and Gauvin, R. (1997) *Polym. Eng. Sci*., 37(5), 757–771.
13. Rouison, D., Sain, Mohini and Couturier, M. (2003) *J. Appl. Polym. Sci*., 89(9), 2553–2561.
14. Kenny, J.M., Maffezzoli, A. and Nicolais, L. (1990) *Compos. Sci. Technol*., 38(4), 339–358.
15. Kiuna, N., Lawrence, C.J., Fontana, Q.P.V., Lee, P.D., Selerland, T. and Spelt, P.D.M. (2002) *Compos. Part A: Appl. Sci*., 33(11), 1497–1503.
16. Rudd, C.D., Long, A.C., Kendall, K.N. and Mangin, C.G.E. Liquid Molding Technologies, Woodhead Publ.: Cambridge, England, 1997.
17. Wang, Y.X. and Ishida, H. (1999) *Polymer*, 40(16), 4563–4570.
18. Liu, X. and Gu, Y. (2002) *J. Appl. Polym. Sci*., 84(6), 1107–1113.
19. Xiang, H., Ling, H., Wang, J., Song, L. and Gu, Y. (2005) *Polym. Compos.,* 26(5), 563–571.
20. Tontisakis, A., Blyakhman, Y. and Chaudhari, A. New high performance RTM system, 49th SAMPE International Symposium, Long Beach, CA, May, 2004.
21. Ning, X. and Ishida, H. (1994) *J. Polym. Sci. A Chem. Ed.,* 32(6), 1121–1129.
22. Reghunadhan, C.P. (2004) *Prog. Polym. Sci.*, 29, 401–498.
23. Shen, S.B. and Ishida, H. (1996) *Polym. Compos*., 17(5), 710–719.
24. Gu, Y., Ran, Q.C. and Tian, Q. Study on properties of benzoxazine containing aldehyde group, the 14th National Conference on Composite Materials, China, 193–196, October, 2006.
25. Ran, Q.C., Tian, Q. and Gu, Y. (2006) *Chinese Chem. Lett*., 17(10), 1305–1308.
26. Gu, Aijuan. (2005) *Polym. Adv. Technol*., 16, 563–566.
27. Halley, P.J. and Mackay, M.E. (1996) *Polym. Eng. Sci.,* 36(5), 593–609.
28. Yousefi, A., Lafleur, P.G. and Gauvin, R. (1997) *Polym. Compos*., 18(2), 157–168.
29. Liang, Z.Y., Duan, Y.X., Lin, Y., Fan, X.Y. and Zhang, Z.G. (2001) *Acta Mater. Compos. Sinica*, 18, 16–19.
30. Rimdusit, S. and Ishida, H. (2002) *Rheol. Acta*., 41(1), 1–9.
31. Su, Y.C., Yei, D.R. and Chang, F.C. (2005) *J. Appl. Polym. Sci*., 95(3), 730–737.
32. Jubsilp, C., Damrongsakkul, S., Takeichi, T. and Rimdusit, S. (2006) *Thermochim. Acta*, 447(2), 131–140.
33. Hu, R.Z. and Shi, Q.Z. Thermal Analysis Kinetics, Science Press: Beijing, China, 6, 2001.
34. Ishida, H. and Rodriguez, Y. (1995) *Polymer*, 36(16), 3151–3158.
35. Ishida, H. and Sanders, D.P. (2000) *Macromolecules*, 33(22), 8149–8157.